MYCOBIOLOGY
2021, VOL. 49, NO. 3, 258–266
https://doi.org/10.1080/12298093.2021.1926122

RESEARCH ARTICLE

OPEN ACCESS Check for updates

Unveiling the Functions of the VosA-VelB Target Gene *vidD* in *Aspergillus nidulans*

Ye-Eun Son[a] and Hee-Soo Park[a,b]

[a]School of Food Science and Biotechnology, Kyungpook National University, Daegu, Republic of Korea; [b]Department of Integrative Biology, Kyungpook National University, Daegu, Republic of Korea

ABSTRACT

The *velvet* regulators VosA and VelB are primarily involved in spore maturation and dormancy. Previous studies found that the VosA-VelB hetero-complex coordinates certain target genes that are related to fungal differentiation and conidial maturation in *Aspergillus nidulans*. Here, we characterized the VosA/VelB-inhibited developmental gene *vidD* in *A. nidulans*. Phenotypic analyses demonstrated that the *vidD* deleted mutant exhibited defect fungal growth, a reduced number of conidia, and delayed formation of sexual fruiting bodies. The deletion of *vidD* decreased the amount of conidial trehalose, increased the sensitivity against heat stress, and reduced the conidial viability. Moreover, the absence of *vidD* resulted in increased production of sterigmatocystin. Together, these results show that VidD is required for proper fungal growth, development, and sterigmatocystin production in *A. nidulans*.

ARTICLE HISTORY
Received 4 March 2021
Revised 29 April 2021
Accepted 3 May 2021

KEYWORDS
Velvet; VosA; VelB; asexual development; cleistothecium

1. Introduction

Aspergillus nidulans is a model organism, widely used to understand the reproduction and secondary metabolism of filamentous fungi [1,2]. *Aspergillus nidulans* reproduces asexually or sexually, forming developmental-specific structures during the process [3–5]. During asexual development, *A. nidulans* forms conidiophores, which bear asexual spores (called conidia), and the processes of conidiophore formation are tightly regulated by developmental-specific transcription factors such as BrlA, AbaA, and WetA [6]. *A. nidulans* also form a specialized sexual structure called cleistothecium, which contains sexual spores called ascospores. The regulatory process of fungal development is associated with secondary metabolism in fungi [7]. The results obtained in *A. nidulans* provide the basic knowledge for understanding other *Aspergillus* species such as *A. fumigatus*, *A. flavus*, and *A. oryzae* [8].

The velvet family proteins are fungus-specific transcription factors that coordinate fungal development and secondary metabolism [9]. The velvet family proteins consist of four members: VeA, VelB, VelC, and VosA in *A. nidulans*, containing the DNA-binding velvet domain [10]. In particular, these proteins perform different functions depending on the composition of the complex [10]. For example, the VeA-VelB-LaeA complex coordinates sterigmatocystin (ST) production and sexual development [11]. Another velvet complex, the VosA-VelB complex is a key controller for spore maturation, stress tolerance, and spore germination in *A. nidulans* [12,13]. Because the velvet proteins have a DNA-binding activity, research for the target genes of the VosA-VelB complex has been conducted in spores [14]. These studies primarily focused on the roles of the VosA-VelB complex in spores. Throughout transcriptome analyses, a variety of VosA and VelB target genes have been identified in *A. nidulans* conidia. These include spore-specific genes or developmental-specific genes with known function. Moreover, there are the VosA/VelB-activated developmental (VAD) and the VosA/VelB-inhibited developmental (VID) genes whose function is not known yet.

Several VID or VAD genes were recently characterized in *A. nidulans* [15,16]. The VadA (VosA/VelB-activated developmental gene) has been demonstrated to be a regulator controlling fungal development, spore viability, conidial maturation, stress tolerance, and secondary metabolism in *A. nidulans* conidia [16]. In addition, the VidA (VosA/VelB-inhibited developmental gene) has been shown to be a putative transcription factor, crucial for governing appropriate fungal growth, the balance between asexual and sexual development, and spore formation in *A. nidulans* [15]. The function of two potential *vid* genes, *zcfA*, and *dnjA*, were also studied

CONTACT Hee-Soo Park phsoo97@knu.ac.kr

Table 1. *Aspergillus* strains used in this study.

Strain name	Relevant genotype	References
FGSC4	*A. nidulans* wild type	FGSC[a]
RJMP1.59	*pyrG89; pyroA4*	[19]
TNJ36	*pyrG89; AfupyrG*$^{+}$; *pyroA4*	[20]
TYE6.1 ~ 3	*pyrG89; pyroA4; ΔvidD::AfupyrG*$^{+}$	This study
TYE30.1	*pyrG89; pyroA4::vidD(p)::vidD::FLAG*$_{3x}$*::pyroA*[b]*; ΔvidD::AfupyrG*$^{+}$	This study

[a]Fungal Genetic Stock Center; [b]the 3/4 *pyroA* marker causes targeted integration at the *pyroA* locus.

[17,18]. Some direct target genes of VosA/VelB complex have been disclosed, but there are still genes that have not yet been investigated. In this study, we unveiled the characters of the gene *vidD* in *A. nidulans*.

2. Materials and methods

2.1. Strains, media, and culture conditions

Aspergillus nidulans strains used in this study are described in Table 1. Fungal strains were grown on solid or liquid minimal media (MM) [21]. Colony photographs were taken with a Pentax MX-1 digital camera (Ricoh Imaging Company LTD, Tokyo, Japan). Photomicrographs were taken using a Zeiss Lab A1 microscope (Carl Zeiss MicroImaging GmbH, Jena, Germany) equipped with AxioCam 105c (Carl Zeiss MicroImaging GmbH, Jena, Germany) and AxioVision (Rel. 4.9) digital imaging software (Carl Zeiss MicroImaging GmbH, Jena, Germany). *Escherichia coli* DH5α was grown in Luria-Bertani medium (BD, Sparks MD, USA) with ampicillin (100 μm/mL, Sigma-Aldrich, St. Louis MO, USA) for plasmid manipulation. For auxotrophic strains, uracil/uridine (Acros Organics, Geel, Belgium) or pyridoxine (Sigma-Aldrich, St. Louis MO, USA) were used for cultivation.

2.2. Construction of the vidD deletion mutant strain

The oligonucleotides used in this study are listed in Table 2. To generate the deletion mutant strains, the double-joint PCR strategy was explored as previously described [22]. The 5′ and 3′ flanking regions of *vidD* were amplified from genomic DNA of *A. nidulans* FGSC4 using the primer pair OHS0281:OHS0283 and OHS0282:OHS0284, respectively. The *A. fumigatus pyrG* marker was amplified with OHS0089:OHS0090 from *A. fumigatus* AF293 genomic DNA. Three PCR constructs, including 5′-, 3′-flanking fragments and the *AfupyrG* marker, were joined, and the final cassette was amplified using the primer set OHS0285:OHS0286. The gene deletion cassette was introduced into *A. nidulans* RJMP1.59 protoplasts generated by the Vinoflow FCE lysing enzyme (Novozyme, Bagsvaerd, Denmark). The transformed cells were cultured in the selectable media (MM without uridine or uracil), and at least three mutants were confirmed by PCR followed by restriction enzyme digestion.

2.3. Generation of vidD complementary strain

To generate complement strains, the predicted promoter region and open reading frame of each gene were amplified using the primer pair OHS0914:OHS0460 from *A. nidulans* FGSC4 genomic DNA. The PCR constructs were digested with *Not*I and cloned to pHS13 [23]. The resulting plasmid pYE5.1 for *vidD* was introduced into TYE6.1 protoplast to give rise to TYE30.1. The transformed cells were cultured in the selectable MM and the complementary candidates were confirmed by PCR and quantitative PCR (qPCR) analyses.

2.4. Reverse transcription- qPCR (RT-qPCR) analysis

The samples were prepared as previously described [24]. For vegetative samples, two-day grown conidia of wild type (WT) strain were incubated in liquid MM at 37 °C for 12 or 18 h. Next, the mycelia were collected, washed, squeeze-dried, and stored at −80 °C until RNA isolation. For asexual developmental samples, grown mycelia in liquid MM at 37 °C for 18 h were collected, washed, and transferred to solid MM plates. The plates were incubated at 37 °C and samples were collected at the designated time points, squeeze-dried, and stored −80 °C until RNA isolation. For conidia samples, 2-day cultures of controls and mutant strains were collected and stored −80 °C.

Total RNA isolation was carried out as previously described [17]. Each sample was homogenized in 1 mL of TRIzol reagent (Invitrogen, Waltham, MA, USA) using a Mini-Bead Beater (BioSpec Products, Bartlesville, OK, USA) and 0.3 mL of Zirconia/Silica beads (RPI, Mt. Prospect, IL, USA). The supernatant was mixed with an equal volume of iced isopropanol and centrifuged again. The RNA pellets were washed with 70% ethanol by diethyl pyrocarbonate (DEPC) treated water and dissolved in RNase-free water. To remove genomic DNA contamination, the samples were treated with the RQ1 RNase-Free DNase (Promega, Madison, WI, USA), and then

Table 2. Oligonucleotides used in this study.

Name	Sequence (5′→3′)[a]	Purpose
OHS0089	GCTGAAGTCATGATACAGGCCAAA	5′ *AfupyrG* marker_F
OHS0090	ATCGTCGGGAGGTATTGTCGTCAC	3′ *AfupyrG* marker_R
OHS0281	ATCAGACTCAGAGTGCCGTCC	5′ *vidD* DF
OHS0282	GCCGAAGGAGGGGTAATCAAT	3′ *vidD* DR
OHS0283	*GGCTTTGGCCTGTATCATGACTTCA* TATCGCAAGAGCATGAATATCG	3′ *vidD* with *AfupyrG* tail
OHS0284	*TTTGGTGACGACAATACCTCCCGAC* GCACAACCAGACAGTACCTTGG	5′ *vidD* with *AfupyrG* tail
OHS0285	ACACATCTTCGTGCCCACCT	5′ *vidD* NF
OHS0286	GCGCTATTTCTGGCATAGGCG	3′ *vidD* NR
OHS0914	aatt **GCGGCCGC** CTCTTCGCACACCGAGG	5′ *vidD* with promoter_*Not*I
OHS0460	aatt **GCGGCCGC** GGCAGTTCGCTTTCGCAG	3′ *vidD* with *Not*I
OHS0449	CCACCGAAGAGGATGCCATA	5′ *vidD* RT_F
OHS0450	AGATCCACTTGCCGAGAGAG	3′ *vidD* RT_R
OHS0576	GGTTGAAGTCGTCGGTTGAG	5′ *tpsA* RT_F
OHS0577	TGGAAACCGATGAGGTCACA	3′ *tpsA* RT_R
OHS0616	CTCCTACTCGCGTCACTTCT	5′ *orlA* RT_F
OHS0617	AGGAAAGACATCCACAGCCA	3′ *orlA* RT_R

[a]Tail sequences are shown in italics. Restriction enzyme sites are in bold.

RNA was purified using the RNeasy Mini Kit (Qiagen, Hilden, Germany). RNA concentration and quality were measured by the absorbance of ultraviolet (UV) using Eppendorf BioSpectrometer, (Eppendorf AG, Hamburg, Germany). Complementary DNA (cDNA) was synthesized using reverse transcriptase (Promega, Madison, WI, USA) and qPCR was carried out using CFX96 Touch Real-Time PCR (Bio-Rad, Hercules, CA, USA) and iTaq Universal SYBR Green Supermix. To calculate the expression levels of target genes, the $2^{-\Delta\Delta CT}$ method was used and the β-actin gene was used as the endogenous control [25,26]. Primer sets for qPCR are listed in Table 2.

2.5. Conidial trehalose analysis

The conidial trehalose assay was performed as previously described [27]. Two-day-old conidia (2×10^8) of control and mutant strains were collected, washed with ddH_2O, resuspended in ddH_2O, and incubated at 95 °C for 20 min. The supernatant was collected after centrifugation, transferred to a new tube, and mixed with an equal volume of 0.2 M sodium citrate (pH 5.5). The samples were incubated at 37 °C for 8 h with or without trehalase (3 mU, Sigma, St. Louis, MO, USA), hydrolyzing trehalose to glucose. The amount of glucose generated from the trehalose was assayed with a Glucose Assay Kit (Sigma, St. Louis, MO, USA).

2.6. Conidia viability assay

Conidia viability was determined as described previously [17,27]. Fresh conidia (10^5 per plate) of WT and mutant strains were spread onto solid MM and incubated at 37 °C. After 2 or 10 days, the conidia were collected and counted using a hemocytometer. Approximately 100 conidia were spread onto solid MM and incubated for 2 days at 37 °C in triplicate. Survival rates were calculated as the ratio of the number of viable colonies relative to the number of spores inoculated.

2.7. Thermal tolerance assay

Thermal tolerance test was carried out as previously described [13] with minor modifications. About 1×10^3 conidia cultured for 2 days were incubated at 55 °C for 15 or 30 min. Approximately 100 conidia of control and mutant strains were spread onto solid MM. After the plates were incubated at 37 °C for 48 h, the number of colonies was counted. The survival rates were calculated as the ratio of the number of viable colonies to the number of untreated control colonies, in triplicates.

2.8. Phenotypic analysis of cleistothecium

To examine the sexual structures, control and mutant strains were incubated on solid sexual medium (SM) at 37 °C for 7 or 21 days under dark conditions. After culture, plates were washed with 95% ethanol. Next, photographs of cleistothecia were taken using a Zeiss Lab.A1 microscope and the size of cleistothecia was measured using AxioVision (Rel. 4.9) digital imaging software.

The number of germinated ascospores in cleistothecium was recorded as previously described [28]. Control and mutant strains were inoculated onto SM for 7 or 21 days, and 10 individual cleistothecia were separated from the plates and washed with ddH_2O. After being transferred to a new tube in 100 μL of ddH_2O, samples were diluted three times. The diluted samples were spread into MM agar plates, incubated at 37 °C for 2 days, and then the numbers of colonies were counted. All experiments were performed in triplicates.

2.9. Sterigmatocystin extraction and thin-layer chromatography

The ST extraction was carried out as previously described [29]. Conidia ($\sim 10^5$) of each strain were

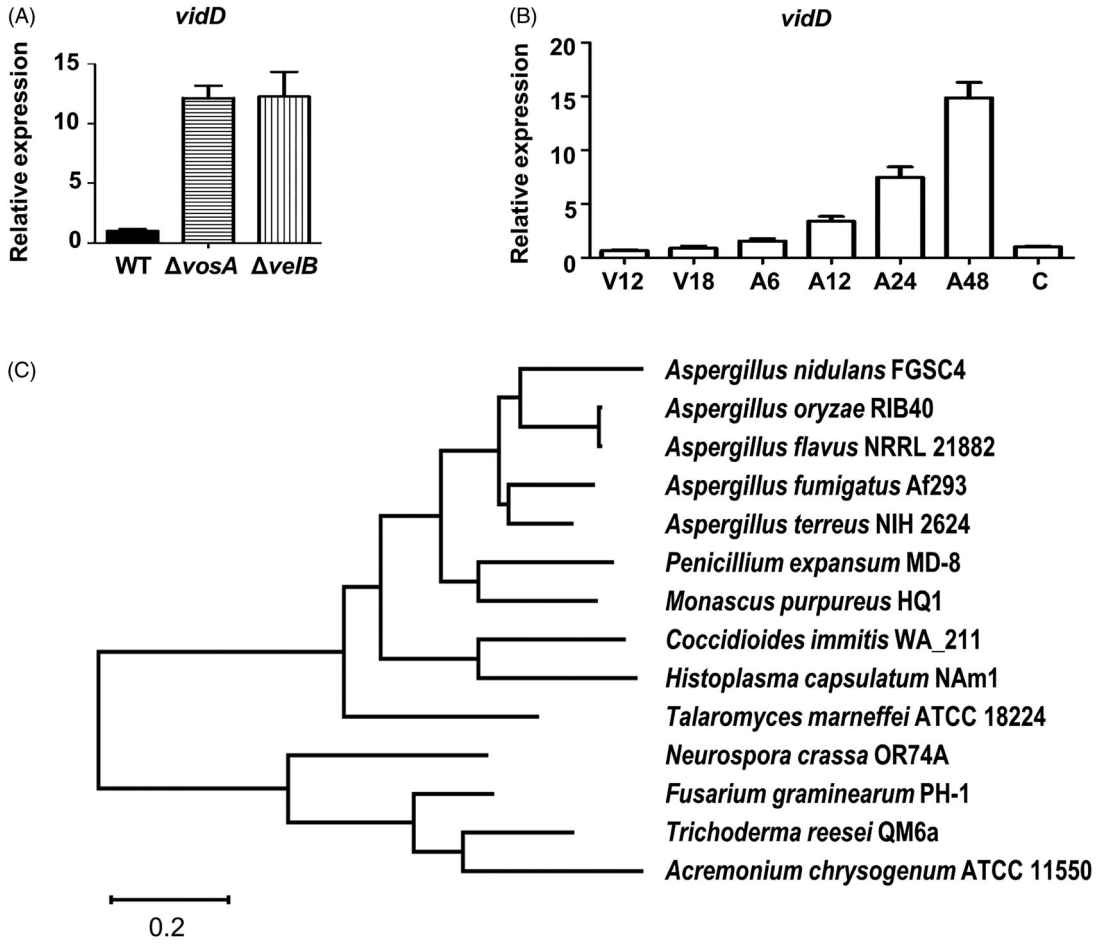

Figure 1. Summary of *vidD*. (A) Relative mRNA expression level of *vidD* was measured in wild-type (WT), Δ*vosA,* and Δ*velB* conidia. (B) The mRNA level of *vidD* was measured during the life cycle of WT. V: vegetative growth, A: post asexual developmental induction, C: conidia. (C) A phylogenetic tree of VidD homolog proteins identified in ascomycetes including *Aspergillus nidulans* FGSC4 (XP_664463), *A. terreus* NIH2624 (XP_001211143), *A. oryzae* RIB40 (XP_023092531), *A. fumigatus* Af293 (XP_753347), *A. flavus* NRRL 21882 (RAQ43558), *Talaromyces marneffei* ATCC 18224 (XP_002145337), *Penicillium expansum* MD-8 (XP_016598290), *Neurospora crassa* OR74A (XP_011394950), *Coccidioides immitis* WA_211 (TPX23157), *Histoplasma capsulatus* NAm1 (XP_001543235), *Fusarium graminearum* PH1 (XP_011320485), *Monascus purpureus* HQ1 (TQB68067), *Trichoderma reesei* QM6a (XP_006965184), and *Acremonium chrysogenum* ATCC 11550 (KFH47513). A phylogenetic tree of VidD-like proteins was generated by MEGAX software (http://www.megasoftware.net/) using the alignment data from ClustalW2 and the maximum likelihood method based on the JTT matrix-based model. The bootstrap consensus tree inferred from 1000 replicates is taken to represent the evolutionary history of the taxa analyzed.

inoculated into 5 mL of liquid complete medium and cultured at 30 °C for 7 days under dark conditions. After incubation, an equal amount of $CHCl_3$ was added per sample. Samples were centrifuged for 10 min. The separated organic phase was transferred to new glass vials and evaporated using an oven. Samples were resuspended in 100 μL of $CHCl_3$ and loaded into a thin-layer chromatography (TLC) silica plate with a fluorescence indicator (Kiesel gel 60, 0.25 mm; Merck, Burlington, MA, USA). The plate was developed in toluene:ethyl acetate:acetic acid (8:1:1, v/v/v), treated with 1% aluminum hydroxide hydrate (Sigma, St. Louis, MO, USA), and baked at 95 °C for 1 min. TLC plate images were captured with exposure to UV (366 nm). The spot intensities of the ST were quantified using Image J software. Experiments were performed in triplicates for each strain.

2.10. Statistical analysis

Statistical differences between control and Δ*vidD* strains were evaluated by Student's unpaired *t*-test. Mean ± SD are shown. *P*-values < 0.05 were considered to be significant.

3. Results

3.1. Summary of vidD

vidD (*AN6859*) is a putative VosA/VelB-inhibited developmental gene in *A. nidulans* conidia [9]. To verify whether VosA and VelB affect the expression of *vidD* in conidia, we checked the levels of *vidD* mRNA in WT, Δ*vosA*, and Δ*velB* conidia. As shown in Figure 1(A), mRNA expression of *vidD* increased >10-fold in Δ*vosA* and Δ*velB* conidia compared with WT conidia. Next, we checked the *vidD*

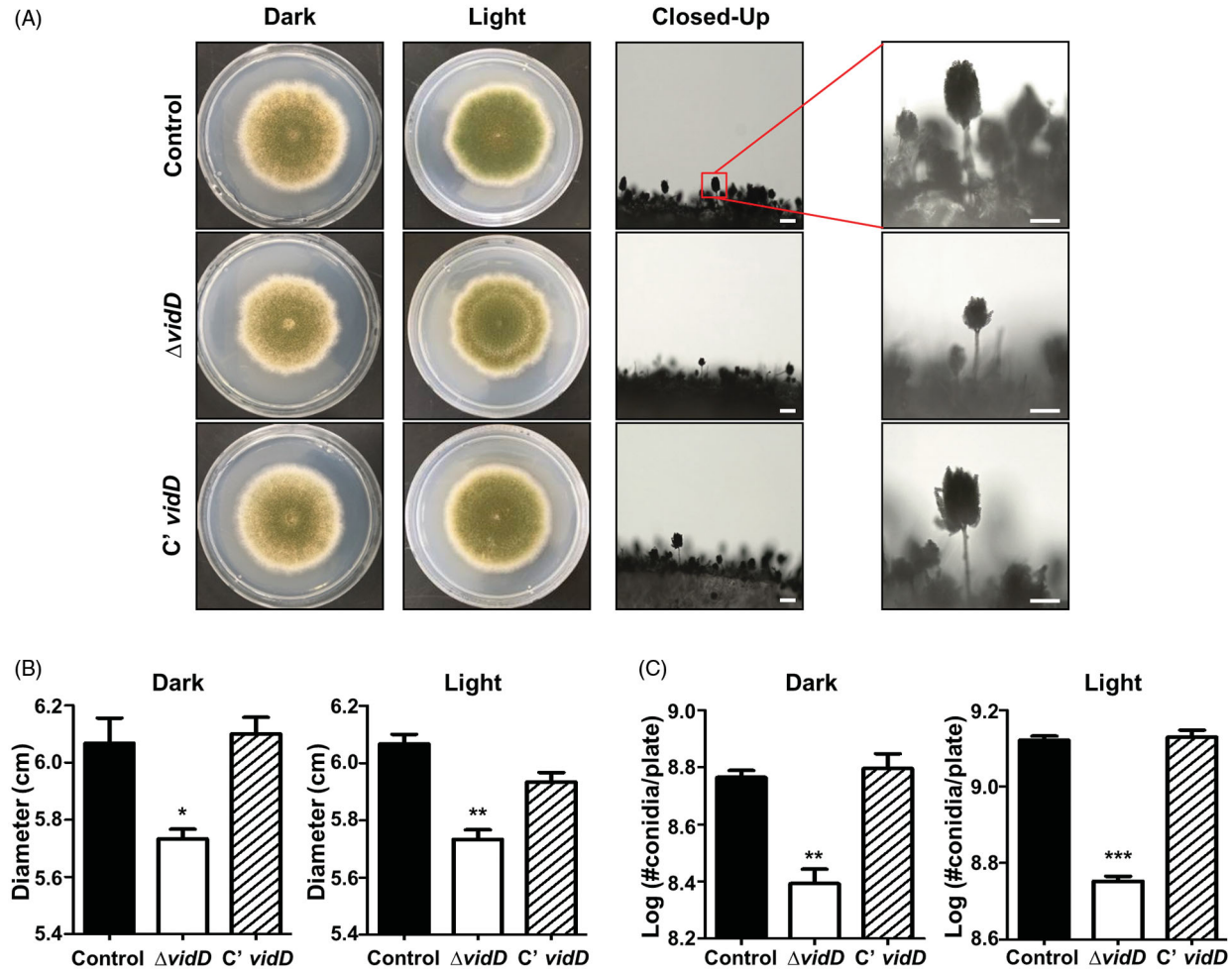

Figure 2. Phenotypic analysis of asexual development in the Δ*vidD* mutant. (A) Colony photographs of control (TNJ36), Δ*vidD* (TYE6.1), and C′ *vidD* (TYE30.1) strains that were point-inoculated on solid MM plate and grown at 37 °C for 5 days under dark or light conditions. The right panel shows conidiophores of control (TNJ36), Δ*vidD* (TYE6.1), and C′ *vidD* (TYE30.1) observed under the microscope after 48 h of cultivation (bar = 0.25 μm). (B) Quantitative analysis of colony diameter for control (TNJ36), Δ*vidD* (TYE6.1) and C′ *vidD* (TYE30.1) shown in (A) ($^{**}p < 0.01$, $^{*}p < 0.05$). (C) Quantitative analysis of asexual spore production of the strains shown in (A) ($^{***}p < 0.001$, $^{**}p < 0.01$). All experiments were carried out in triplicates.

mRNA level during vegetative growth and asexual development. The mRNA level of *vidD* was increased during post asexual developmental induction, but rapidly decreased in the conidia (Figure 1(B)). The *vidD* gene encodes a polypeptide consisting of 309 amino acids, but it does not contain a known domain. Next, we checked the VidD homolog in fungal systems. The VidD homolog was found in most Pezizomycotina fungi, including all *Aspergillus* species, but not in Saccharomycotina fungi, such as *Saccharomyces cerevisiae* and *Candida albicans*, and Basidiomycota, such as *Cryptococcus neoformans* and *Ustilago maydis* (Figure 1(C)).

3.2. Deletion of vidD affects fungal growth and development

To investigate the roles of VidD, the control, *vidD* deletion mutant, and C' strains were point-inoculated onto solid MM plates and incubated under dark or light conditions for 7 days. As shown in Figure 2(A), the Δ*vidD* null mutant produces abnormal, light green conidia compared with the control and C' strains. The colony diameter was smaller than that of control and C' strains (Figure 2(B)). In addition, the number of conidia produced by Δ*vidD* mutant was lower than that of WT and C' strains under both dark and light conditions (Figure 2(C)). These results suggest that VidD is required for appropriate fungal growth and conidial formation in *A. nidulans*.

Next, we studied the function of VidD in sexual development by inoculating each strain onto SM for 7 and 21 days under dark conditions. After 7 days of cultivation, the Δ*vidD* mutant produced either immature cleistothecia (Figure 3(A)) or the size of the mature cleistothecia of Δ*vidD* were smaller than that of control and C' strain (Figure 3(B)). In addition, the mature cleistothecium of Δ*vidD* contains fewer germinating ascospores compared with control and C' strains (Figure 3(C)). At 21 days, the Δ*vidD* mutant produced mature cleistothecia, but these cleistothecia were smaller in size than cleistothecia of control and C' strains (Figures 3(D,E)). The

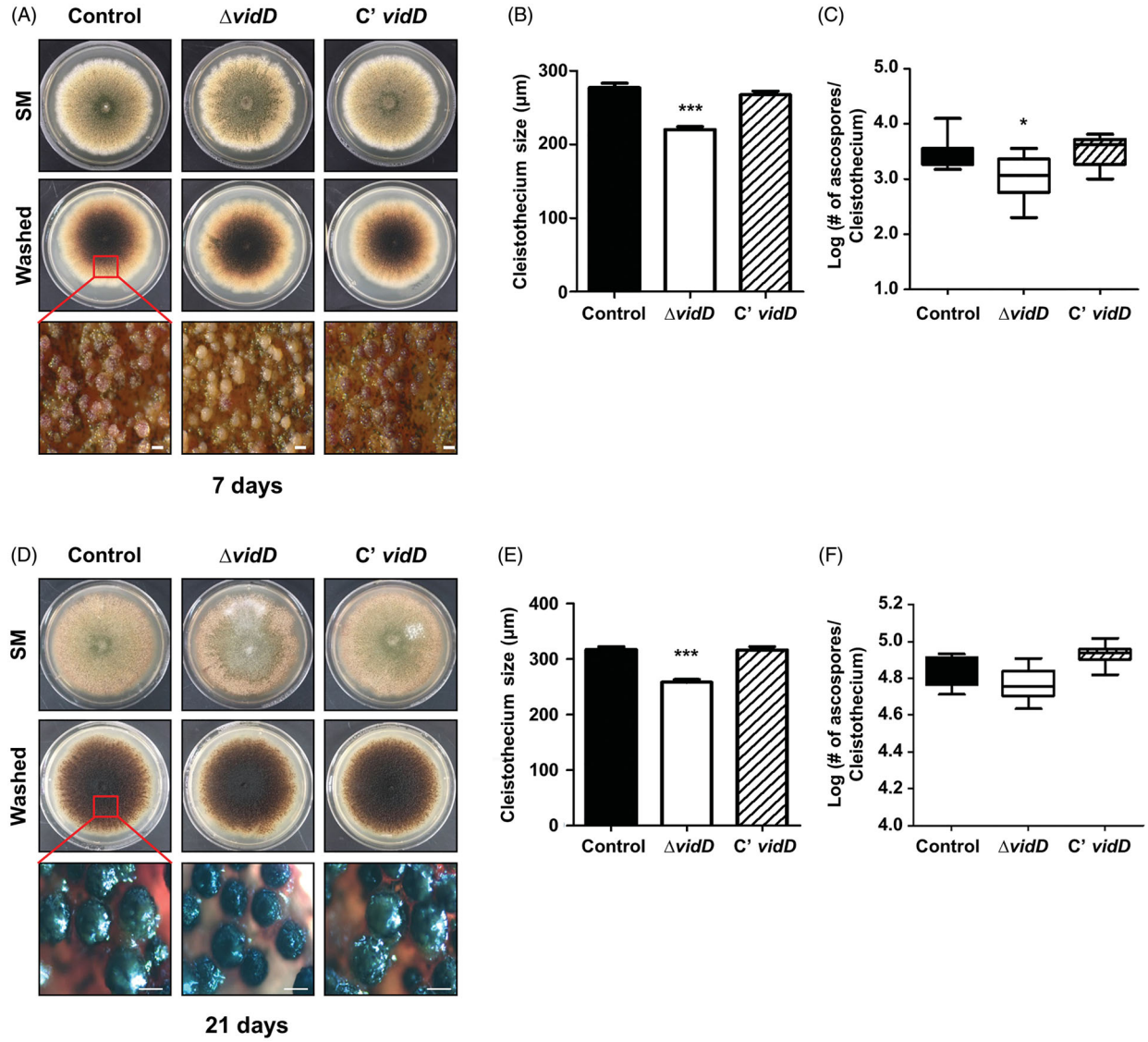

Figure 3. Sexual developmental phenotypes of the Δ*vidD* mutant. (A) Phenotypic analysis of control (TNJ36), Δ*vidD* (TYE6.1), and C′ *vidD* (TYE30.1) strains inoculated onto solid sexual media (SM) and incubated at 37 °C for 7 days under dark conditions. Bottom panel shows the cleistothecia observed by microscopy after washing off the conidia. (B) Quantitative analysis of cleistothecium size for shown in (A) ($^{***}p < 0.001$). (C) Quantitative analysis of the number of germinating ascospores per cleistothecium in strains shown in (A) ($^{*}p < 0.05$). (D) Phenotypic analysis of control (TNJ36), Δ*vidD* (TYE6.1), and C′ *vidD* (TYE30.1) strains inoculated onto solid SM and incubated at 37 °C for 21 days in the dark condition. Bottom panel shows the cleistothecia observed by microscope after washing off the conidia. (E) Quantitative analysis of cleistothecium size for strains shown in (D) ($^{***}p < 0.001$). (F) Quantitative analysis of the number of germinating ascospores per cleistothecium in strains shown in (D).

cleistothecium of the Δ*vidD* mutant contains an almost similar number of germinating ascospores (Figure 3(F)). Overall, these results indicated that VidD is essential for appropriate sexual development in *A. nidulans*.

3.3. The role of VidD in conidia

The VosA/VelB complex regulates trehalose contents of conidia and spore viability in *Aspergillus* species [30]. To investigate whether VidD affects trehalose biosynthesis, we measured the amount of trehalose in the Δ*vidD* conidia. As shown in Figure 4(A), trehalose contents in the Δ*vidD* conidia are less than that of control and C' *vidD* conidia. Next, we examined mRNA expression of the *tpsA* and *orlA* genes associated with trehalose biosynthesis. The levels of *tpsA* and *orlA* mRNA slightly decreased in Δ*vidD* conidia compared with control and C' *vidD* conidia (Figure 4(B)), suggesting that VidD is required for proper trehalose biosynthesis.

Because trehalose is an important disaccharide for spore viability and protection against environmental stresses in fungi [31,32], we assayed conidial viability and thermal tolerance in conidia. Conidial viability of the Δ*vidD* mutant was decreased compared with that of control and C' *vidD* strains (Figure 4(C)). In addition, Δ*vidD* conidia are more sensitive to thermal stress (Figure 4(D)). Together, these data demonstrated that VidD is an essential

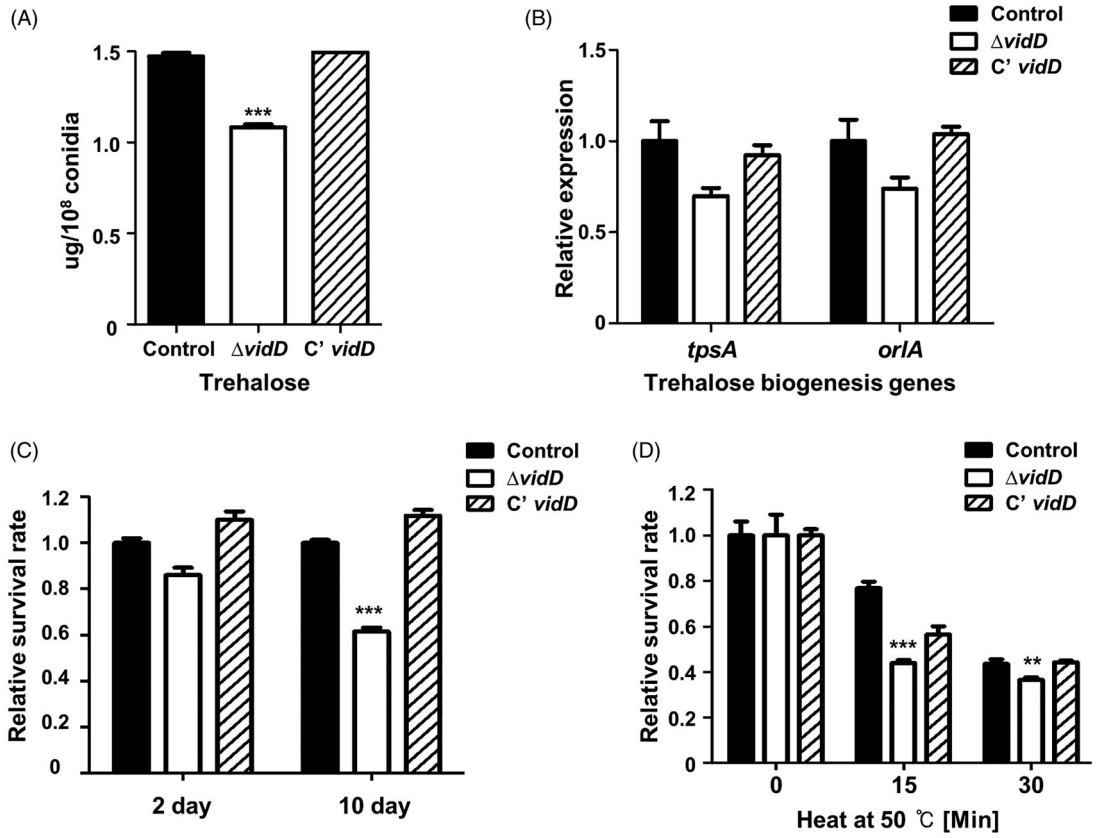

Figure 4. The roles of VidD in conidia. (A) The amount of trehalose per 10^8 conidia from 2-days cultures of control (TNJ36), Δ*vidD* (TYE6.1), and C′ *vidD* (TYE30.1) (***$p < 0.001$). (B) The mRNA levels of *tpsA* and *orlA* in control (TNJ36), Δ*vidD* (TYE6.1) and C′ *vidD* (TYE30.1) conidia. (C) Conidia viability for control (TNJ36), Δ*vidD* (TYE6.1), and C′ *vidD* (TYE30.1) strains grown at 37 °C for 2 and 10 days (***$p < 0.001$). (D) Thermal stress tolerance of conidia from control (TNJ36), Δ*vidD* (TYE6.1), and C′ *vidD* (TYE30.1) strains. About 100 conidia were incubated at 50 °C for 0, 15, and 30 min and spread into solid MM (***$p < 0.001$, **$p < 0.01$).

regulator of trehalose biosynthesis and thermal stress tolerance.

3.4. Deletion of vidD affects sterigmatocystin production

To investigate whether VidD affects sterigmatocystin production, we extracted sterigmatocystin from control, Δ*vidD*, and C' *vidD* strains and spotted extracted samples onto TLC plates with sterigmatocystin as a standard. The absence of *vidD* produces a higher amount of ST compared with WT and C' strains (Figure 5). This result implies that VidD is required for proper sterigmatocystin production.

4. Discussion

The VosA-VelB hetero-complex is a key protein-complex for spore maturation, dormancy, and germination [12,23]. In addition, the VosA-VelB complex regulates transcript expression of spore-specific or developmental-specific genes in *A. nidulans* conidia [14]. Previously, we identified a variety of VosA (or VelB) target genes, *vadA*, *vidA*, *zcfA*, and *dnjA* in *A. nidulans* [15–18]. These genes are involved in asexual/sexual development, sterigmatocystin production, and conidia maturation. In this study, we characterized *vidD*, another VosA/VelB-inhibited developmental gene in *A. nidulans*. Deletion of *vidD* led to the formation of abnormal conidiospores and decreased conidia production. Moreover, the absence of *vidD* caused the delayed formation of sexual fruiting bodies and decreased germination ability of ascospores. Based on these results, we can speculate that VidD is a developmental regulator affecting both asexual and sexual development. In addition, VidD can affect the production of sterigmatocystin in *A. nidulans*.

Another finding is that VidD might be a potential fungal specific protein. The result of sequence similarity searching indicated that the VidD homologs were found in most Ascomycota. However, the VidD homologs could not be found in Hemiascomycota (*S. cerevisiae* and *C. albicans*), Zygomycota (*Mucor circinelloides* and *Rhizopus oryzae*), Basidiomycota (*C. neoformans* and *U. maydis*), animals, and plants. This implies that VidD can act as the fungus-specific protein in growth, development, and sterigmatocystin production. Although the cellular role of *vidD* was characterized in this study, the molecular role of *vidD* has not been studied. As a result of domain analysis, VidD does

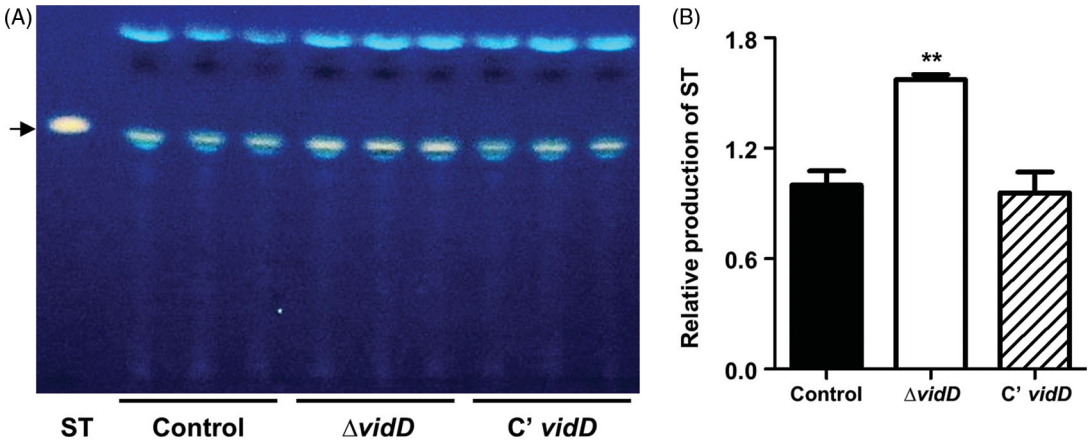

Figure 5. Sterigmatocystin production in the Δ*vidD* mutant. (A) Thin-layer chromatography (TLC) plate image of sterigmatocystin (ST) generated by control (TNJ36), Δ*vidD* (TYE6.1) and C′ *vidD* (TYE30.1) strains. The arrow indicates ST. (B) Relative production of ST produced after 7 days in the dark (**$p < 0.01$). Experiments were carried out in triplicates.

not contain a known domain, which makes it difficult to predict the molecular function of VidD. Therefore, further study will be needed to characterize the molecular role of VidD.

In conclusion, we characterized the developmental role of VidD in *A. nidulans*. Deletion of *vidD* affects colony growth, production of conidiophores, formation of sexual fruiting bodies, conidial maturation, and sterigmatocystin accumulation, implying that VidD plays multi-functional roles in *A. nidulans*. Additional studies will provide insight into detailed molecular mechanisms of VidD in other fungal species

Disclosure statement

No potential conflict of interest was reported by the author(s).

Funding

The work was financially supported by a National Research Foundation of Korea (NRF) grant to HSP, funded by the Korean government [NRF-2020R1C1C1004473].

References

[1] Etxebeste O, Espeso EA. *Aspergillus nidulans* in the post-genomic era: a top-model filamentous fungus for the study of signaling and homeostasis mechanisms. Int Microbiol. 2020;23(1):5–22.
[2] McCluskey K, Baker SE. Diverse data supports the transition of filamentous fungal model organisms into the post-genomics era. Mycology. 2017;8:67–83.
[3] Adams TH, Wieser JK, Yu J-H. Asexual sporulation in *Aspergillus nidulans*. Microbiol Mol Biol Rev. 1998;62(1):35–54.
[4] Dyer PS, O'Gorman CM. Sexual development and cryptic sexuality in fungi: insights from *Aspergillus* species. FEMS Microbiol Rev. 2012;36:165–192.
[5] Krijgsheld P, Bleichrodt R, van Veluw GJ, et al. Development in *Aspergillus*. Stud Mycol. 2013;74:1–29.
[6] Park H-S, Yu J-H. Genetic control of asexual sporulation in filamentous fungi. Curr Opin Microbiol. 2012a;15:669–677.
[7] Han KH. Molecular genetics of *Emericella nidulans* sexual development. Mycobiology. 2009;37:171–182.
[8] Galagan JE, Calvo SE, Cuomo C, et al. Sequencing of *Aspergillus nidulans* and comparative analysis with *A. fumigatus* and *A. oryzae*. Nature. 2005;438:1105–1115.
[9] Ahmed YL, Gerke J, Park HS, et al. The velvet family of fungal regulators contains a DNA-binding domain structurally similar to NF-kappaB. PLoS Biol. 2013;11:e1001750.
[10] Bayram O, Braus GH. Coordination of secondary metabolism and development in fungi: the velvet family of regulatory proteins. FEMS Microbiol Rev. 2012;36:1–24.
[11] Bayram O, Krappmann S, Ni M, et al. VelB/VeA/LaeA complex coordinates light signal with fungal development and secondary metabolism. Science. 2008;320:1504–1506.
[12] Park HS, Yu YM, Lee MK, et al. Velvet-mediated repression of beta-glucan synthesis in *Aspergillus nidulans* spores. Sci Rep. 2015;5:10199.
[13] Sarikaya Bayram O, Bayram O, Valerius O, et al. LaeA control of *velvet* family regulatory proteins for light-dependent development and fungal cell-type specificity. PLoS Genet. 2010;6:e1001226.
[14] Wu MY, Mead ME, Lee MK, et al. Transcriptomic, protein-DNA interaction, and metabolomic studies of VosA, VelB, and WetA in *Aspergillus nidulans* asexual spores. mBio. 2021;12(1):e03128.
[15] Kim MJ, Jung WH, Son YE, et al. The velvet repressed *vidA* gene plays a key role in governing development in *Aspergillus nidulans*. J Microbiol. 2019;57:893–899.
[16] Park HS, Lee MK, Kim SC, et al. The role of VosA/VelB-activated developmental gene *vadA* in *Aspergillus nidulans*. PLoS One. 2017;12:e0177099.
[17] Son YE, Cho HJ, Chen W, et al. The role of the VosA-repressed *dnjA* gene in development and

metabolism in *Aspergillus* species. Curr Genet. 2020;66:621–633.
[18] Son YE, Cho HJ, Lee MK, et al. Characterizing the role of Zn cluster family transcription factor ZcfA in governing development in two *Aspergillus* species. PLoS One. 2020;15:e0228643.
[19] Shaaban MI, Bok JW, Lauer C, et al. Suppressor mutagenesis identifies a velvet complex remediator of *Aspergillus nidulans* secondary metabolism. Eukaryot Cell. 2010;9:1816–1824.
[20] Kwon NJ, Shin KS, Yu JH. Characterization of the developmental regulator FlbE in *Aspergillus fumigatus* and *Aspergillus nidulans*. Fungal Genet Biol. 2010;47:981–993.
[21] Park H-S, Yu J-H. Multi-copy genetic screen in *Aspergillus nidulans*. Methods Mol Biol. 2012b;944: 183–190.
[22] Yu JH, Hamari Z, Han KH, et al. Double-joint PCR: a PCR-based molecular tool for gene manipulations in filamentous fungi. Fungal Genet Biol. 2004;41(11):973–981.
[23] Park H-S, Ni M, Jeong KC, et al. The role, interaction and regulation of the *velvet* regulator VelB in *Aspergillus nidulans*. PLoS One. 2012;7:e45935.
[24] Park HS, Nam TY, Han KH, et al. VelC positively controls sexual development in *Aspergillus nidulans*. PLoS One. 2014;9:e89883.
[25] Semighini CP, Marins M, Goldman MH, et al. Quantitative analysis of the relative transcript levels of ABC transporter *Atr* genes in *Aspergillus nidulans* by real-time reverse transcription-PCR assay. Appl Environ Microbiol. 2002;68:1351–1357.
[26] Song HY, Choi D, Han DM, et al. A novel rapid fungal promoter analysis system using the phosphopantetheinyl transferase gene, *npgA*, in *Aspergillus nidulans*. Mycobiology. 2018;46: 429–439.
[27] Ni M, Yu J-H. A novel regulator couples sporogenesis and trehalose biogenesis in *Aspergillus nidulans*. PLoS One. 2007;2:e970.
[28] Kim MJ, Lee MK, Pham HQ, et al. The velvet regulator VosA governs survival and secondary metabolism of sexual spores in *Aspergillus nidulans*. Genes. 2020;11(1):103.
[29] Son SH, Son YE, Cho HJ, et al. Homeobox proteins are essential for fungal differentiation and secondary metabolism in *Aspergillus nidulans*. Sci Rep. 2020a;10:6094.
[30] Park H-S, Yu J-H. Velvet regulators in *Aspergillus* spp. Microbiol Biotechnol Lett. 2016;44(4): 409–419.
[31] Fillinger S, Chaveroche MK, van Dijck P, et al. Trehalose is required for the acquisition of tolerance to a variety of stresses in the filamentous fungus *Aspergillus nidulans*. Microbiology. 2001;147: 1851–1862.
[32] Thammahong A, Puttikamonkul S, Perfect JR, et al. Central role of the trehalose biosynthesis pathway in the pathogenesis of human fungal infections: opportunities and challenges for therapeutic development. Microbiol Mol Biol Rev. 2017; 81(2):e00053.